

# Evaluation of the WAMME model surface fluxes using results from the AMMA land-surface model intercomparison project

Aaron Anthony Boone · Isabelle Pocard-Leclercq ·  
Yongkang Xue · Jinming Feng · Patricia de Rosnay

Received: 13 March 2009 / Accepted: 13 August 2009  
© Springer-Verlag 2009

**Abstract** The West African monsoon (WAM) circulation and intensity have been shown to be influenced by the land surface in numerous numerical studies using regional scale and global scale atmospheric climate models (RCMs and GCMs, respectively) over the last several decades. The atmosphere–land surface interactions are modulated by the magnitude of the north–south gradient of the low level moist static energy, which is highly correlated with the steep latitudinal gradients of the vegetation characteristics and coverage, land use, and soil properties over this zone. The African Multidisciplinary Monsoon Analysis (AMMA) has organised comprehensive activities in data collection and modelling to further investigate the significance land–atmosphere feedbacks. Surface energy fluxes simulated by an ensemble of land surface models from AMMA Land-surface Model Intercomparison Project (ALMIP) have been used as a proxy for the best estimate of the “real world” values in order to evaluate GCM and

RCM simulations under the auspices of the West African Monsoon Modelling Experiment (WAMME) project, since such large-scale observations do not exist. The ALMIP models have been forced in off-line mode using forcing based on a mixture of satellite, observational, and numerical weather prediction data. The ALMIP models were found to agree well over the region where land–atmosphere coupling is deemed to be most important (notably the Sahel), with a high signal to noise ratio (generally from 0.7 to 0.9) in the ensemble and a inter-model coefficient of variation between 5 and 15%. Most of the WAMME models simulated spatially averaged net radiation values over West Africa which were consistent with the ALMIP estimates, however, the partitioning of this energy between sensible and latent heat fluxes was significantly different: WAMME models tended to simulate larger (by nearly a factor of two) monthly latent heat fluxes than ALMIP. This results due to a positive precipitation bias in the WAMME models and a northward displacement of the monsoon in most of the GCMs and RCMs. Another key feature not found in the WAMME models is peak seasonal latent heat fluxes during the monsoon retreat (approximately a month after the peak precipitation rates) from soil water stores. This is likely related to the WAMME northward bias of the latent heat flux gradient during the WAM onset.

---

This paper is a contribution to the special issue on West African Climate, consisting of papers from the African Multidisciplinary Monsoon Analysis (AMMA) and West African Monsoon Modeling and Evaluation (WAMME) projects, and coordinated by Y. Xue and P. M. Ruti.

---

A. A. Boone (✉)  
GAME-CNRM, Météo-France, Toulouse, France  
e-mail: aaron.boone@meteo.fr; aaron.a.boone@gmail.com

I. Pocard-Leclercq  
LETG-Géolittomer, Université de Nantes, Nantes, France

Y. Xue · J. Feng  
University of California at Los Angeles, Los Angeles, CA, USA

P. de Rosnay  
European Centre for Medium Range Weather Forecasting,  
Reading, UK

**Keywords** WAM · ALMIP · AMMA · WAMME ·  
Monsoon · Surface fluxes

## 1 Introduction

The West African Monsoon (WAM) circulation intensity and extent are theorised to be significantly interconnected with the land surface. The overall circulation is driven by

land–sea thermal contrast, and the atmosphere–land surface interactions are modulated by the magnitude of the associated north–south gradient of the low level moist static energy (MSE; Eltahir and Gong 1996). The boundary layer MSE gradient exerts a strong influence on the position of the tropical front and the African Easterly Jet (Parker et al. 2005), and therefore the northward penetration of precipitation and its intensity (Philippon and Fontaine 2002). The MSE distribution is a reflection of the surface turbulent fluxes which are highly correlated with the steep latitudinal gradients of the vegetation characteristics and coverage, land use, and soil properties over this zone.

Land surface processes have been shown to have an influence on the West African monsoon (WAM) circulation in numerous numerical studies using regional scale and global scale atmospheric climate models (RCMs and GCMs, respectively) over the last several decades. Charney et al. (1975) was one of the first researchers to use a coupled land–surface atmosphere model to demonstrate a proposed positive feedback mechanism between decreasing vegetation cover and the increase in drought conditions across the Sahel region of Western Africa. Numerous modelling studies since have examined the influence of the land surface on the WAM in terms of surface albedo (e.g. Sud and Fennessy 1982; Laval and Picon 1986), and the vegetation spatial distribution (e.g. Xue and Shukla 1996; Xue et al. 2004; Kang et al. 2007; Li et al. 2007). In addition, Zeng et al. (1999) used an idealised GCM configuration to show a significant contribution of vegetation dynamics to the WAM inter-annual precipitation variability.

The influence of soil moisture (which controls the partitioning of energy between the surface latent and sensible heat fluxes) on the WAM has also been examined using GCMs (e.g. Walker and Rowntree 1977; Cunnington and Rowntree 1986; Rowell and Blondin 1990; Douville et al. 2001). The emphasis on the role of soil moisture is related to the fact that this relatively slow temporally varying component of the coupled land–atmosphere monsoon system theoretically holds promise for improving long range predictability of the WAM. However, this long-term memory effect was recently put into question using a GCM and observational data (Douville et al. 2007), so further study is needed. Indeed there are significant differences with respect to the strength of this coupling simulated by state-of-the-art GCMs over western Africa and elsewhere (Koster et al. 2006; Guo et al. 2006), so the exploration of coupling should be done using a multi-model approach when possible. Part of this discrepancy is probably related to differences in the parameterisations of the surface fluxes and near-surface hydrology in land surface models (LSMs).

The African Multidisciplinary Monsoon Analysis (AMMA) has organised comprehensive activities in data

collection and modelling to further investigate land–atmosphere feedbacks (Redelsperger et al. 2006). In terms of large scale atmospheric multi-model initiatives, the AMMA-Model Intercomparison Project (AMMA-MIP: Hourdin et al. 2009) inter-compares GCMs and RCMs over a meridional transect in West Africa focusing on seasonal prediction. The West African Monsoon Modelling Experiment (WAMME) project utilises such models to address issues regarding the role of ocean–land–aerosol–atmosphere interactions on WAM development (see Xue et al., this issue). The modelling of the land surface component of the WAM is being addressed by the AMMA Land-surface Model Intercomparison Project (ALMIP: Boone et al. 2009). The main idea behind ALMIP is to force a number of state-of-the-art LSMs off-line (i.e. de-coupled from atmospheric models) with the best quality and highest (space and time) resolution data available in order to better understand the key processes and their corresponding scales.

In recent years, there have been a number of offline multi-model intercomparison projects on an international level. Of note is the Project for the Intercomparison of Land-surface Parameterisation Schemes (PILPS: Henderson-Sellers et al. 1995). It dealt with land surface processes at the local to the regional scale and lead to significant improvements in LSM parameterisations. The Global Soil Wetness Project Phase 2 (GSWP-2: Dirmeyer et al. 2006) was an “off-line” global-scale LSM inter-comparison study which produced the equivalent of a land-surface re-analysis consisting in 10-year global data sets of soil moisture, surface fluxes, and related hydrological quantities. The advantage of such offline products is that biases in fully coupled models, notably in terms of precipitation and downwelling radiative fluxes, can be reduced by merging LSM forcing with observational and satellite-based data. The output data sets (notably soil moisture and surface fluxes) have been used as the best estimate of “truth” in numerous recent GCM and RCM studies at the global and regional scales. For example over Africa, Douville et al. (2001) assimilated offline-simulated soil moisture from GSWP-1 (Dirmeyer et al. 1999) into a GCM to study WAM surface–atmosphere feedback mechanisms.

ALMIP is similar to the aforementioned projects, but focuses on the west-African region and it covers the AMMA field campaign time period (the intensive observational phase or IOP was from 2004 to 2006). For example, ALMIP model outputs have recently been used to evaluate the impact of improved land surface physics on the simulation of the WAM by an RCM (Steiner et al. 2009). The main objective of this paper, therefore, is to utilise the off-line simulations of the surface energy fluxes from ALMIP as a proxy for the best estimate of observations in order to evaluate the corresponding fluxes simulated by the fully coupled (land–atmosphere) WAMME models. In this

paper, Sect. 2 describes the ALMIP input data and gives details about the LSM ensemble average, the WAMME-ALMIP surface flux comparison is given in Sect. 3, and conclusions and perspectives are given in Sect. 4.

## 2 Creation of the ALMIP surface flux dataset

### 2.1 ALMIP input forcing and parameters

The land surface model forcing database is comprised of two components, one for the land surface parameters, and the other for the LSM upper boundary conditions consisting in the atmospheric state variables, precipitation and downwelling radiative fluxes from multiple sources. The ECOCLIMAP global database (Masson et al. 2003) provides land surface parameters (albedo, vegetation cover fraction, surface roughness, leaf area index, soil texture, etc.). The vegetation phenology corresponds to a single representative annual at a 10-day time step. The default spatial resolution is 1 km, and included software up-scales and interpolates the data to the desired grid projection and spatial resolution. It is intended for use by LSMs in offline mode or which are coupled to GCM, numerical weather prediction (NWP), mesoscale meteorological research or hydrological models.

The low level atmospheric state variables are derived from the European Centre for Medium Range Weather Forecasts (ECMWF) forecasts from 2001 to 2007 at a 3 h time step. Downwelling radiative fluxes from OSI-SAF (Oceans and Ice Satellite Applications Facility: <http://www.osi-saf.org>) for 2004 and the LAND-SAF fluxes (Land Satellite Applications Facility: Geiger et al. 2008) for 2005–2007 are substituted for the corresponding NWP fluxes. The Tropical Rainfall Measurement Mission (TRMM) precipitation product 3B-42 (Huffman et al. 2007) is used from 2002 to 2007 (hereafter this product is simply referred to as TRMM in this paper). The TRMM rainfall estimates are based on combined calibrated microwave and infrared precipitation estimates with a rescaling to monthly gauge data where applicable. Note that there are many precipitation products available, but only TRMM met the main requirements of ALMIP-Exp3: (1) the spatial resolution ( $0.25^\circ$ ) was at or higher than that of the simulation grid, (2) the diurnal cycle is resolved (a 3 h time step is used by TRMM), (3) the entire annual cycle over the full LSM integration period is covered, (4) and TRMM was found to give relatively good rainfall estimates over this region in an AMMA-sponsored rainfall product intercomparison study (Jobard et al. 2007), and the best of the products meeting criteria 1–3. It should be noted that the goal of ALMIP is not to create new precipitation products, but rather to test existing datasets.

### 2.2 ALMIP experimental setup

The ALMIP model domain consists in the continental land surface bounded in the region from  $-5^\circ$  to  $20^\circ\text{N}$  longitude, and  $-20^\circ$  to  $30^\circ\text{E}$  latitude at a  $0.50^\circ$  spatial resolution (see Fig. 1). The ALMIP results presented in this paper are from Experiment 3 (hereafter these results are simply referred to as ALMIP in this paper) which uses a merged forcing which was described in the previous section (see Boone et al. 2009, for details on the other ALMIP experiments). Nine LSMs ran this experiment which covered the time period from 2002 to 2007, and they are listed along with a recent reference in Table 1. There were a total of 11 LSM simulations (two models did simulations using two different options: ISBA used the force-restore and the multi-layer diffusion soil options, while ORCHIDEE lowered the minimum allowable soil moisture from the default value). All of the LSMs used the same grid and atmospheric forcing, and the majority of the LSMs used either the provided soil and vegetation parameters or the closest equivalents, while a few used their own set of parameters (e.g. the ECMWF model used ALMIP results to test the influence of soil moisture initialisation in their operational forecast system, so they used their own set of parameters).

### 2.3 ALMIP ensemble average

Gao and Dirmeyer (2006) showed the advantages and improved realism of using a multi-LSM model average of simulated surface properties. They presented several different weighting techniques, ranging from a simple average to one using optimised weights which minimised errors based on observations. The low spatial density of surface observations over West Africa precluded the use of optimised weights, so the simple ensemble-mean of the ALMIP simulated surface fluxes are used in this study (which was also shown by Gao and Dirmeyer 2006, to be preferable to any single model realisation).

The evapotranspiration, *Evap*, for each LSM averaged over the core WAM season (June–September: JJAS) for 2005 is shown in Fig. 1. The northward extent and gradient of *Evap* is quite similar among the LSMs and is controlled to a large extent by the precipitation in this water-stressed region (north of about  $15^\circ\text{N}$ ). While there are some differences around  $10^\circ\text{N}$ , the most significant differences are located over the equatorial forest region (east of  $10^\circ\text{E}$ , and south of  $5^\circ\text{N}$ ). Because the inter-LSM differences in surface fluxes for the two ISBA and ORCHIDEE sensitivity runs were considerably smaller than the overall inter-LSM scatter (compare Fig. 1a, b, g, h, respectively), their results were simply averaged to give single realisation for these two models resulting in a 9-member ensemble average (denoted as AVG in Fig. 11).

**Fig. 1** ALMIP model evapotranspiration (*Evap*) averaged from May through October (the period covered by the WAMME model outputs) for 2005. The ALMIP ensemble average is shown in panel l

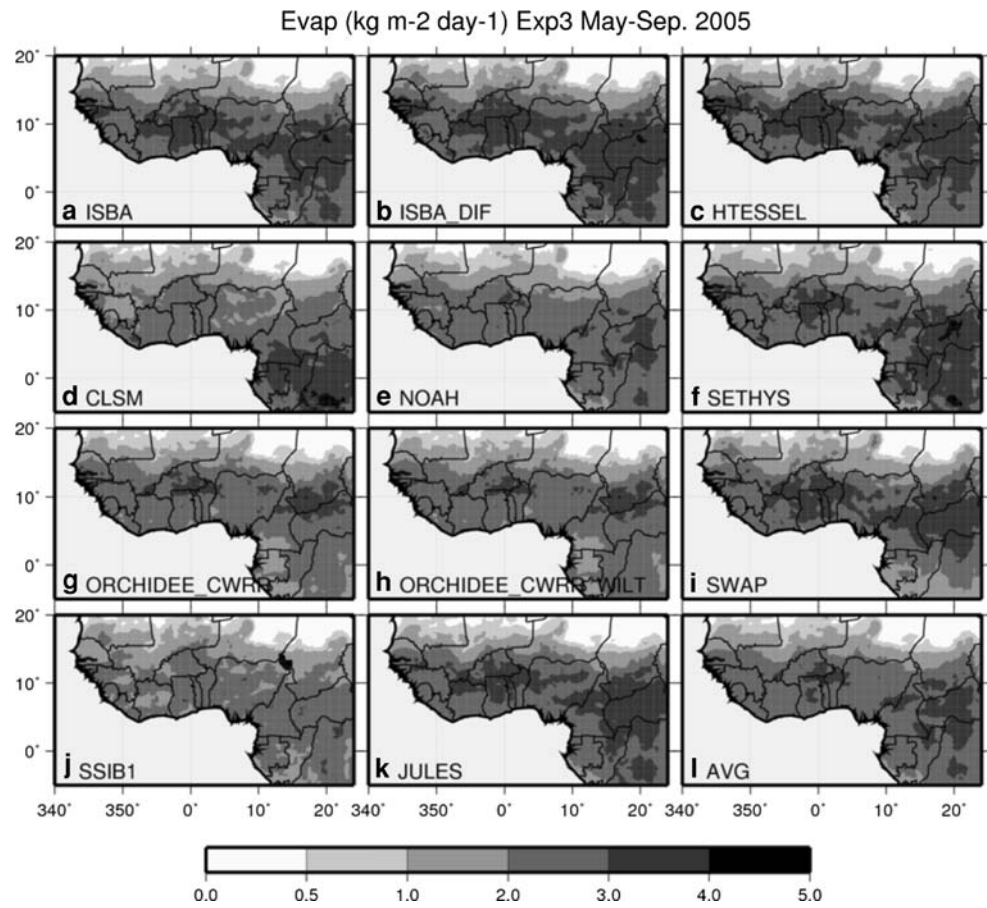


**Table 1** ALMIP Exp.3 models

Model Acronym	Institute	Recent references	ALMIP model configuration
HTESSEL	ECMWF, Reading, UK <i>G. Balsamo</i>	Balsamo et al. (2009)	4L, 6 tiles, 1E, SV: ECMWF
ORCHIDEE-CWRR	IPSL, Paris, France T. Orgeval and <i>P. deRosnay</i>	d'Orgeval et al. (2008), de Rosnay et al. (2002)	11L, 13 tiles, 1E, SV: ECOCLIMAP
ISBA <sup>a</sup> ISBA-DIF <sup>b</sup>	CNRM, Météo-France, Toulouse <i>A. Boone</i>	(a) Noilhan and Mahfouf (1996), (b) Boone et al. (2000)	3L <sup>a</sup> , 5L <sup>b</sup> , 1 tile, 1E, SV: ECOCLIMAP
JULES	CEH, Wallingford, UK <i>P. Harris</i>	Essery et al. (2003)	4L, 9 tiles, 1E, SV: ECOCLIMAP
SETHYS	CETP/LSCE, France <i>S. Saux- Piccard and C. Ottlé</i>	Coudert et al. (2006)	2L, 12 tiles, 2E, SV: ECOCLIMAP
NOAH	CETP/LSCE (NCEP) <i>B. Decharme and C. Ottlé</i>	Chen and Dudhia (2001), Decharme (2007)	7L, 12 tiles, 1E, SV: ECOCLIMAP
CLSM	UPMC, Paris, France <i>S. Gascoïn and A. Ducharne</i>	Koster et al. (2000)	5L, 5 tiles, 3E, SV: ECOCLIMAP
SSiB	LETG, Nantes, France; UCLA, Los Angeles, USA <i>I. Pocard- Leclercq</i>	Xue et al. (1991)	3L, 1 tile, 2E, SV: SSiB
SWAP	IWP, Moscow, Russia <i>Y. Gusev and O. Nasonova</i>	Gusev et al. (2006)	3L, 1 tile, 1E, SV: ECOCLIMAP

A recent model reference is given. The names of the people who performed the simulations are in italics. The model configuration used for ALMIP is shown in the rightmost column where L represents the number of vertical soil layers, E represents the number of energy budgets per tile (a separate budget for snow cover is not considered here), and SV corresponds to the soil–vegetation parameters used. Tile refers to the maximum number of completely independent land surface types permitted within each grid box

Quantitative estimates of the inter-LSM variability are shown in Fig. 2. The so called “omega” statistic (Koster et al. 2002) is used to give an estimate of the signal to noise ratio: it was computed using daily average *Evap* values over the entire annual cycle for 2005 and is shown in Fig. 2a. Large values (approaching unity) indicate areas where the model time series are well correlated, which corresponds to a more significant impact of the forcing (notably the precipitation). The best agreement occurs over the Sahel region (north of about 10°N), which is of interest as this is the region where precipitation recycling should be significant. Areas with lesser LSM agreement (lower values) are located where soils are generally deeper and the vegetation coverage is more dense (especially in forested areas). Several factors lead to greater LSM disagreement here: deeper soils coupled with parameterisation differences in sub-surface hydrology and water uptake by vegetation cause model dispersion, and there is considerable spread in terms of the time evolution of soil evaporation beneath forest canopies.

The coefficient of variation (ratio of the inter-LSM variability to the LSM average) for the same time interval is shown in Fig. 2b. Values are not surprisingly highest along the northern fringe of the domain owing to very low

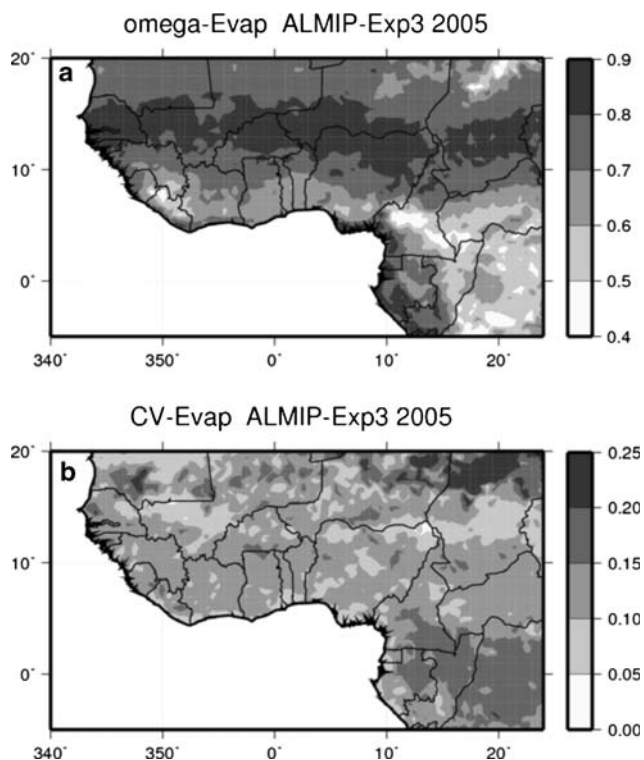


**Fig. 2** The “omega” coefficient, which represents the signal to noise ratio in the ensemble, for the ALMIP *Evap* is shown in panel a, and the coefficient of variation is shown in panel b. Both statistics were computed using daily values for all of 2005

precipitation rates coupled with a very high atmospheric demand, however, elsewhere the inter-LSM variability is about 5–15% of the average which indicates a fairly good agreement. The values are slightly larger (exceeding 15%) over the equatorial forest region. In this paper, however, the lower agreement over the aforementioned zone is not very important as the focus is on the region from –10° to 10°E, where the LSMs have a fairly good agreement.

The monthly LSM-average ( $\pm 1$  SD) water and energy budget components averaged over the Sahel are shown in Figs. 3a and b, respectively. Note that hereafter in this paper, the Sahel is somewhat arbitrarily defined from –10° to 10°E longitude, and from 11° to 17°N latitude. Although the onset of heavier precipitation is earlier in 2005 than in 2004, some general observations can be made for both years. Peak *Evap* occurs approximately 2 months after peak rains (in July), and the timing of this peak corresponds with the change in sign of soil moisture storage (the peak is mostly storage driven). Also, the LSM-average runoff ratio (runoff to precipitation) is rather low (less than approximately 10% over the Sahel) and total annual soil water storage is also a relatively small, so much of the rainfall is recycled (evaporated).

The corresponding LSM surface flux components (net radiation, *Rnet*, sensible, *Qh*, and latent, *Qle*, heat fluxes) are shown in Fig. 3b. The inter-LSM *Rnet* scatter is lower

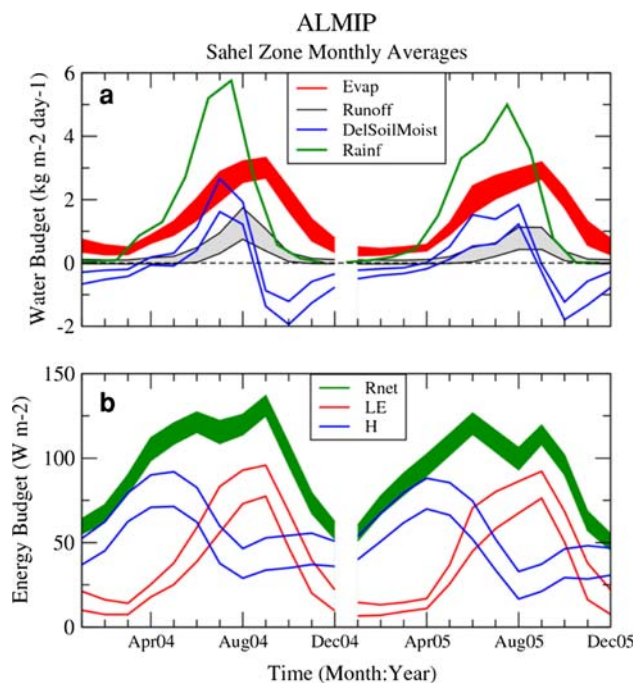


**Fig. 3** The mean and spread ( $\pm 1$  SD) for the ALMIP ensemble computed over the Sahel (see the text for the definition of the Sahel used herein). The water budget components are shown in panel a, and the energy budget components are shown in panel b

than for the surface turbulent fluxes, which results because most of this flux is constrained by the forcing (incoming shortwave and longwave fluxes are the same for all models, and in addition the emissivity and albedo are prescribed). In both years, there is a double-peak (maxima in June and September), which result primarily due to high incoming shortwave radiation prior to monsoon onset and just after it's retreat. The sensible and latent heat flux peaks are approximately 5 months apart, with the  $Q_{le}$  becoming dominant during the onset month, and the  $Q_h$  becoming larger at the end of each year once the soil moisture reserve has been sufficiently depleted.

In terms of ALMIP evaluation, it was found that the LSMs performed well on the large scale in terms of capturing the seasonal cycle of the near surface soil moisture using remotely sensed data (see de Rosnay et al. 2009, for details). Many land surface flux stations were installed during the AMMA field campaign (Redelsperger et al. 2006), but it is difficult to compare ALMIP output fluxes directly with local scale values due to the ALMIP grid resolution. However, spatially up-scaled surface fluxes are available for the Mali mesoscale site which corresponds to the ALMIP grid box at  $-1.5^\circ\text{E } 15.5^\circ\text{N}$ . The comparison of the observed up-scaled surface  $Q_h$  with the ALMIP-AVG for a single pixel is shown in Fig. 4. The modelled and observed aggregated  $Q_h$  values have been averaged over 10-day periods for this comparison. The  $Q_h$  time series for each site have been weighted by the fraction of their corresponding land cover type over the mesoscale box (approximately 60 km resolution) using remotely sensed data (Timouk et al. 2008). In Fig. 4, dashed curves correspond to the 3-year average (2005–2007) time series for each observation site within the mesoscale domain. Each site represents a very different land cover type: Kelma is a low-lying marshy site during and after the wet season, Eguerit is a rocky site with little vegetation, and the Agoufou site has sparse low vegetation. The aggregated observed fluxes and associated variability are shown by the shaded region. The solid curves enclose a region bounded by  $\pm 1$  SD about the LSM-AVG  $Q_h$  averaged over 2005–2007. The LSM-average simulated  $Q_h$  response to the wet season and the subsequent dry-down are well correlated with the observed average  $Q_h$ , and the magnitude is well simulated. A detailed analysis of ALMIP LSM evaluation is beyond the scope of this paper (for more details, see Boone et al. 2009).

### 3 WAMME surface flux evaluation

The analysis in this study focuses on the period from 2004 to 2005 because there is an overlap between the WAMME and ALMIP outputs. Note that WAMME also covers 2003,

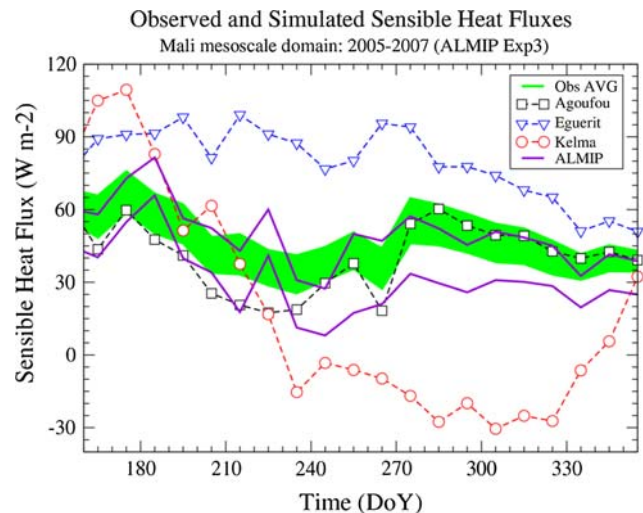


**Fig. 4** The 3-year average (2005–2007) observed  $Q_h$  for the three local sites are indicated by the *dashed lines*, and the *shaded green area* corresponds to the spread of the spatially aggregated fluxes (representing the  $60 \times 60 \text{ km}^2$  supersite domain). The *solid curves* enclose the spread (1 SD) of the ALMIP multi-model  $Q_h$  averaged over 2005–2007 for Exp.3. The observed flux data for this figure were taken from Timouk et al. (2008)

but the satellite-based SAF radiative fluxes were not available for this year. The WAMME evaluation is based on the availability of outputs from May to October. Note that the focus of this study is on seasonal cycles, so that the monthly mean values are examined in this study. Finally, a description of the WAMME models and the experimental setup are given in Xue et al. (this issue); the same model naming convention is used herein. A summary of the WAMME LSM configurations are given in Table 2.

#### 3.1 Comparison of WAMME variables with ALMIP forcing

The precipitation simulation by the WAMME models is of key importance for the surface fluxes, especially in the Sahel where the atmospheric demand and large incoming radiative energy cause most of the precipitation to be evaporated from the surface (as shown in Sect. 2). The WAMME simulated precipitation for the entire ALMIP domain averaged over the core monsoon period JJAS 2004 is compared to the TRMM precipitation in Fig. 5 in the form of scatter plots (the correlation, root mean square difference or RMS and the bias are shown in each panel). The majority of the WAMME models have a positive precipitation bias. NCEP2 (NCEP reanalysis version 2) has one of the lowest at  $-0.1 \text{ kg m}^{-2} \text{ day}^{-1}$ , but NCEP2 replaced model precipitation at the surface with a rainfall product (see Xue et al., this issue). The inter-rainfall product variability for several standard satellite and gauge based products is considerably smaller than the inter model

**Table 2** As in Table 1 except for the WAMME LSMs

WAMME GCM/RCM Acronym	LSM acronym and reference	WAMME configuration
NCEP	NCEP: Pan and Mahrt (1987)	2L, 1 tile, 1E
CFS	NOAH: Chen and Dudhia (2001)	4L, 1 tile, 1E
GFS	NOAH (as above)	4L, 1 tile, 1E
COLA	SSiB: Xue et al. (1991)	3L, 1 tile, 2E
UCLA	SSiB (as above)	3L, 1 tile, 2E
UCLA MRF	SSiB (as above)	3L, 1 tile, 2E
JMA	SiB: Sellers et al. (1986)	3L, 1 tile, 2E
NASA FVGCM	CLM: Dai et al. (2003)	10L, 1 tile, 2E
NCAR CAM	CLM: (as above)	10L, 1 tile, 2E
MOHC	JULES: Essery et al. (2003)	4L, 1 tile, 1E
NASA GMAO	MOSAIC: Koster and Suarez (1996)	3L, 8 tiles, 1E
MM5	NOAH: Chen and Dudhia (2001)	4L, 1 tile, 1E
NASA GISS	GISS: Rosenzweig and Abramopoulos (1997)	6L, 1 tile, 2E
RegCM	BATS: Dickinson et al. (1993)	3L, 1 tile, 2E

A recent model reference is given (the atmospheric model references can be found in Xue et al. 2009). The default LSM configuration used is shown in the rightmost column. The LSMs each used their respective vegetation and soil parameters

variability (see Xue et al., this issue: this is also discussed in more detail in the next paragraph). A high correlation implies that the position and strength of the JJAS-averaged meridional precipitation gradient is similar between the WAMME model and TRMM, and two models (UCLA, and MOHC HadRM3P-NCEP) have both a high correlation (above 0.8) and a relatively low bias (less than  $1 \text{ kg m}^{-2} \text{ day}^{-1}$ ). It is interesting to note that the best statistics overall are obtained by the GCM ensemble (Fig. 5b). The significance of the ensemble performance is detailed in Xue et al. (this issue).

In fact, it should be noted that the results presented here are not exclusive to TRMM. Indeed, the agreement between different commonly used satellite rainfall products at the monthly scale is much better than that among the WAMME models, so any one of several can be used to evaluate the model performances (depending on the spatial and temporal resolution requirements for evaluation). An example is shown for the Sahel in Fig. 6: thick lines correspond to the commonly used products TRMM, Global Precipitation Climatology Centre (GPCP: Schneider et al. 2008), Global Precipitation Climatology Project (GPCP: Adler et al. 2003), and Climate Prediction Center RainFall Estimation version 2.0 (CPC-RFE2: Laws et al. 2004). The thin lines correspond to the WAMME simulated rain rates. Note that the rainfall simulation problem is also present in operational NWP models (the ECMWF curve based on 12–36 h forecasts is also shown, and it underestimates the rainfall primarily because the latitude of the core of the active precipitation zone is south of the Sahel. This problem is well known at ECMWF: A. Beljaars, personal communication).

The spatial correlations of the downwelling shortwave radiation and the precipitation (averaged over JJAS 2004)

are shown in Fig. 7 (where the same letters are used to identify the WAMME models as in Fig. 5). Of the 17 simulations shown, the majority of them show a fair consistency in that better shortwave radiation simulations correspond to better precipitation simulations (compared to the satellite-based product OSI-SAF). Once again, the GCM ensemble is the best (symbol b). Three of the four models with the lowest shortwave correlation tend to simulate the monsoon too far north or south compared to the ALMIP forcing, while the remaining one (NCEP-GFS) simulates a reasonable position but with widespread high precipitation rates within the active monsoon region. Note that the inter-model variability exceeds the inter-annual differences for the 2 years considered, so the conclusions are essentially the same for 2004 as 2005 (not shown here). The spatial and temporal distributions of the precipitation and incoming solar energy obviously modulate the surface fluxes, especially in the transition zone from the desert to vegetated areas (in the Sahel). This will be examined further in the next section.

### 3.2 WAMME simulated surface fluxes

The key surface flux which couples the surface to the atmosphere via the hydrological cycle is the latent heat flux. The WAMME model JJAS average latent heat flux,  $Q_{le}$ , for 2004 is shown in Fig. 8 (the ALMIP  $Q_{le}$  is shown in Fig. 8w). Looking at the spatial patterns and magnitudes, it is seen that the GCM ensemble compares best with ALMIP (consistent with the analysis in the previous section, see Fig. 7). Three models have relatively high  $Q_{le}$  rates up to  $20^\circ\text{N}$  owing to the penetration of the monsoon too far north (MRI-JMA, Cornell MM5, NCAR CAM-CLM3 and MOHC HadAM3), two models have a monsoon

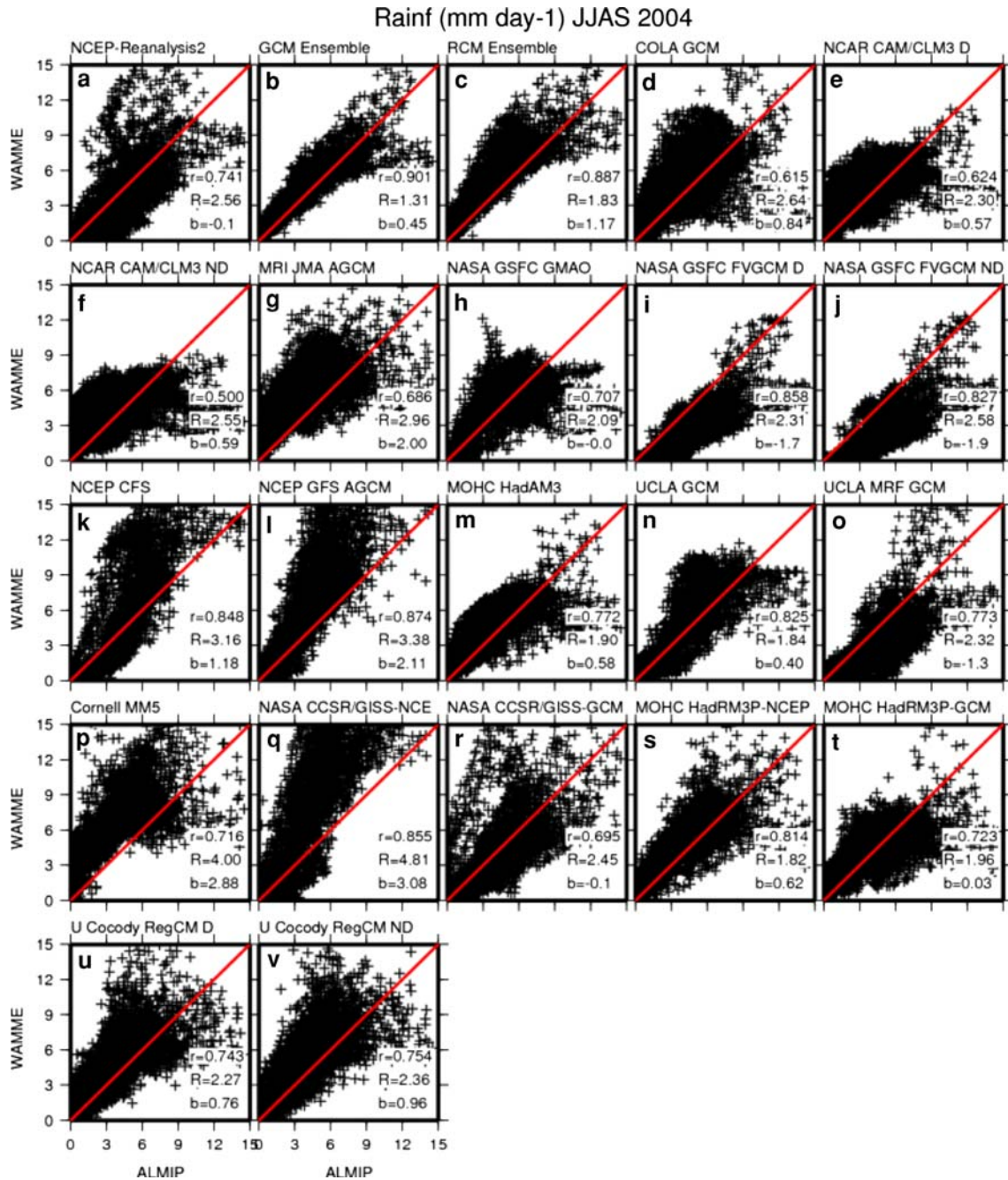


**Fig. 5** Scatter plots of the WAMME simulated rainfall versus the values from ALMIP (based on TRMM 3B42). The statistics are computed over the 4 month core monsoon period (June–September).

The statistics shown are the correlation,  $r$ , the root mean square difference,  $R$ , and the bias,  $b$

which stays too far south (UCLA-MRF and NASA GSFC FVGCM), while the remaining models are more consistent with ALMIP. Because of the significant amount of precipitation recycling north of about 10°N because of large atmospheric demand, the evaporation and precipitation are highly correlated. The meridional  $Q_{le}$  gradient varies significantly among the models, and this will be discussed in more detail later in this section.

The statistical comparison of the JJAS 2004  $Q_{le}$  between the WAMME models and ALMIP is shown in Fig. 9. The lowest bias and root mean square difference is for NCEP2, which is reassuring since the surface received a satellite-based precipitation product as opposed to the model precipitation. The best overall agreement with ALMIP in terms of all three statistics is once again the GCM ensemble, although the RCM ensemble is fairly close.

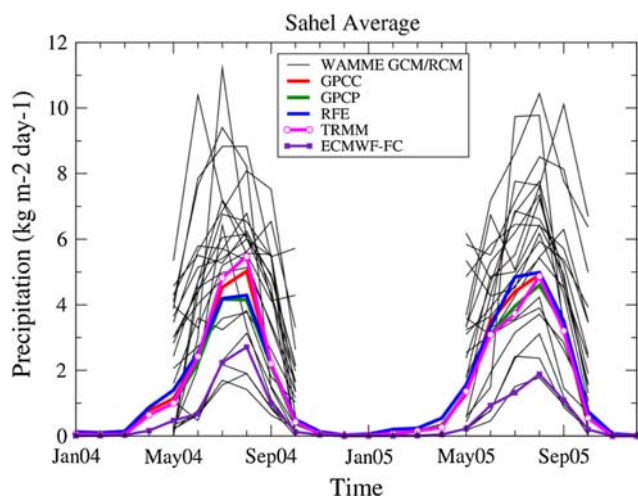


**Fig. 6** Comparison of the spatial correlation between WAMME and ALMIP for the downwelling solar radiation (ordinate) and the precipitation. The boxed region indicates models which performed the best

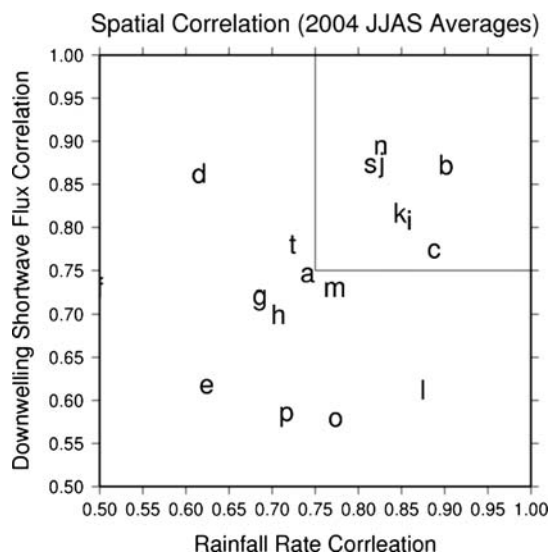


**Fig. 7** The Sahel average rainfall monthly time series for 2 years: different precipitation products are represented by thick curves, and the WAMME model simulations are indicated by the thin black curves. The ECMWF forecast simulation is also indicated

Because of the positive precipitation bias of the WAMME models, there is also a positive  $Q_{le}$  bias with many models having maximum values of approximately 50% larger than ALMIP maximum values. The overall WAMME  $Q_{le}$  positive bias is probably also related to the fact that most of the models tend to simulate the monsoon too far north, where atmospheric demand is larger so that precipitation recycling should be intensified.

Hovmoller plots of  $Q_{le}$  for 2004 (from May to October) are shown in Fig. 10, where the  $Q_{le}$  has been averaged from  $-10^{\circ}$  to  $10^{\circ}$ E longitude. The ALMIP  $Q_{le}$  temporal

evolution is asymmetric, with considerably larger  $Q_{le}$  rates during the monsoon retreat than during any other period. This results as water stored in the root zone is evaporated after the precipitation rates have diminished. The large  $Q_{le}$  results from a combination of ample soil moisture, significant incoming solar radiation and relatively large atmospheric demand (i.e. relatively dry atmospheric conditions). There is also a relative ALMIP  $Q_{le}$  minimum transitioning from July to August south of  $10^{\circ}$  N due to lower precipitation and incoming radiation and humid conditions. In contrast with ALMIP, most of the WAMME models have a fairly symmetric  $Q_{le}$  temporal evolution, with only COLA, MOHC HadAM3, NCEP-GFS, NCAR CAM/CLM3 and Cornell MM5 having maximum  $Q_{le}$  rates occurring during the monsoon retreat. NCEP2 has the best overall agreement in terms of  $Q_{le}$  meridional gradient and northward extent and timing, but this is expected as the precipitation is not from the atmospheric model (it is satellite based as for ALMIP). Therefore for most of the models, the soil water reserve does not seem to be greatly impacting the late season  $Q_{le}$ . In general agreement with ALMIP, most of the models have a relative  $Q_{le}$  minimum south of  $10^{\circ}$ N during the monsoon period, but the exact position in time, magnitude and spatial extent are quite variable.

Of key importance (as mentioned in the introduction) for the monsoon intensity, is the meridional gradient of the surface fluxes. The ratio of  $Q_h$  to the  $R_{net}$  is used in order to explore the surface energetics in a relative sense. The corresponding meridional gradient for each of the WAMME models (averaged from  $-10^{\circ}$  to  $10^{\circ}$ E longitude) for three times (onset in June, peak monsoon activity in August and post monsoon in October) are shown in Fig. 11 together with the ALMIP values. Several WAMME models have been highlighted (using thick curves) as a reference. During the onset period for both years, ALMIP has more energy going into sensible than latent heating compared to WAMME. Again, this is probably mostly related to the lower ALMIP precipitation rates. Also, quite a few models already have the active monsoon region extending up to approximately  $13^{\circ}$ N indicated by the inflection point in many of the curves. Although there is considerable scatter, most of the models are similar to ALMIP in August (except for those which place rainfall north of  $20^{\circ}$ N, indicated by the very low ratios north of  $15^{\circ}$ N). Ratios range from approximately 0.3 to 0.7 from south to north. October has the most inter-model scatter north of about  $12^{\circ}$ N, with ratios ranging from 0.2 to nearly 1.0 at  $20^{\circ}$ N. In contrast, the models have the best agreement with each other and with ALMIP south of  $10^{\circ}$ N. This is probably because the relatively low incoming solar radiation is preferentially used for evaporation over the relatively wet and well vegetated surfaces. One model of note is NCEP2, which has a markedly different behaviour than all of the other

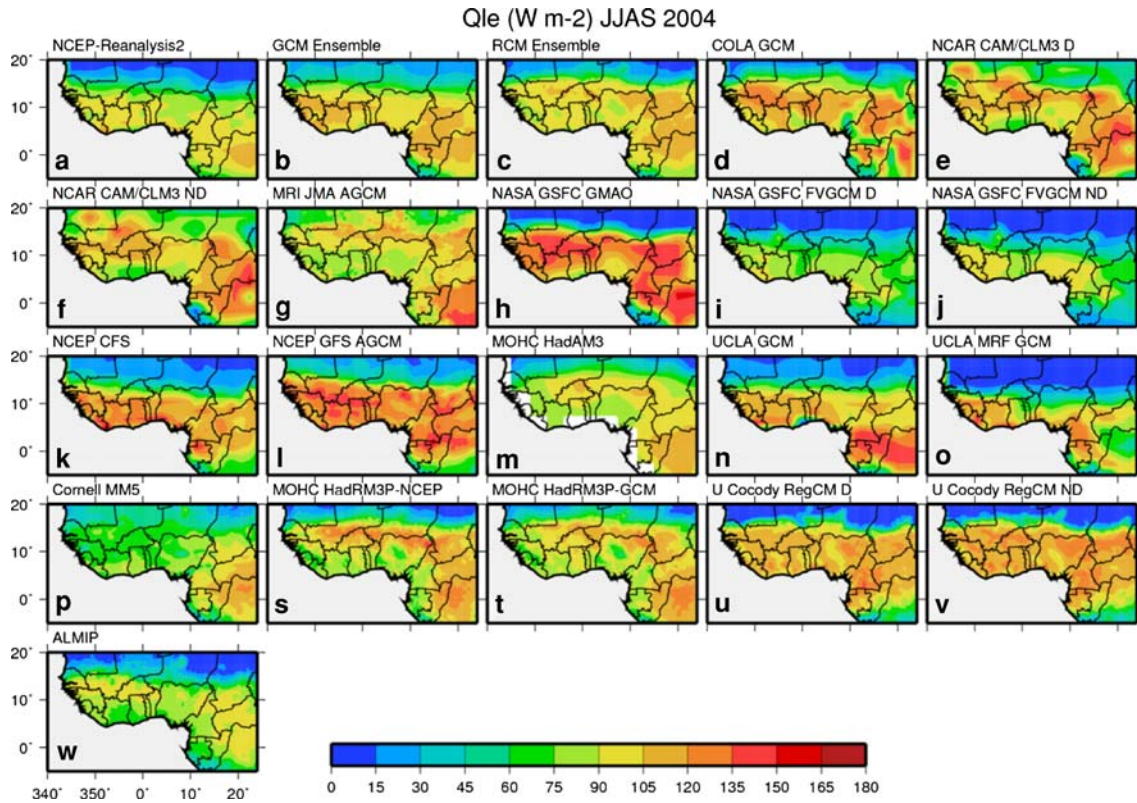


**Fig. 8** The WAMME latent heat flux averaged from June through September (JJAS) for 2004. The corresponding ALMIP field is shown in panel w

models during October north of  $15^{\circ}\text{N}$ . In fact, NCEP2 has a very high desert albedo, and this contributes to a rather low  $R_{\text{net}}$  in this region. Despite the fact that this is anomalous compared to the other models, owing to a lack of observations north of about  $17^{\circ}\text{N}$  it is difficult to say whether or not this behaviour is realistic or not. But the magnitudes of the turbulent fluxes for all of the models are fairly low in this region at this time of year, so the influence on the WAM is likely to be low.

A comparison of the 6-month (May–October) mean surface turbulent fluxes averaged from  $-10^{\circ}$  to  $10^{\circ}\text{E}$  is shown in Fig. 12 for 2004 and 2005. As noted before, the differences between the same WAMME models for the 2 years is far less than the inter-model differences. The diagonal lines represent the value of the ALMIP  $R_{\text{net}}$ , and the boxes represent the range of the ALMIP fluxes. The ALMIP inter-model standard deviation of the turbulent fluxes (not shown) is approximately  $5 \text{ W m}^{-2}$  in 2004 and  $4 \text{ W m}^{-2}$  in 2005 (the ALMIP averages are denoted using **A**), while the corresponding value for the  $R_{\text{net}}$  is approximately  $4 \text{ W m}^{-2}$  for both years. The WAMME  $R_{\text{net}}$  is rather consistent with the ALMIP values for most of the models, although a few models have lower values which are mostly related to higher surface albedo. In terms of partitioning this energy into turbulent fluxes, ALMIP uses

slightly more of the available energy for latent heating (approximately  $60 \text{ W m}^{-2}$  vs. about  $45 \text{ W m}^{-2}$  for sensible heating). Consistent with the previous analyses (the positive WAMME model precipitation bias), the WAMME models use approximately twice the amount of available energy for latent than sensible heating. So it is possible that the coupling or feedback mechanism (via precipitation recycling) is over-estimated in the WAMME models. This question will need to be studied more thoroughly using fully coupled models (Fig. 13).

Soil moisture has a direct influence on the surface turbulent fluxes (and thus PBL development and convection), but as evidenced by many authors, it is very difficult to compare soil moisture diagnostics between different models (see Koster et al. 2009, for a recent comprehensive review of this problem). In the end, since it is not actually the soil moisture that matters to the atmospheric model, but rather its impact on the partitioning of latent and sensible heat fluxes, we have given a measure of SWI (–) meaning proxy in the Fig. 13) based on  $\text{SWI}_p = \text{Qle}/R_{\text{net}}$ . It will be near zero when evaporation is negligible (where soils are nearly completely dry), and it will be large when the soils are relatively moist (above an effective field capacity), so this ratio is directly related to the fluxes felt by the atmosphere. NCEP2 has the most consistent spatial pattern

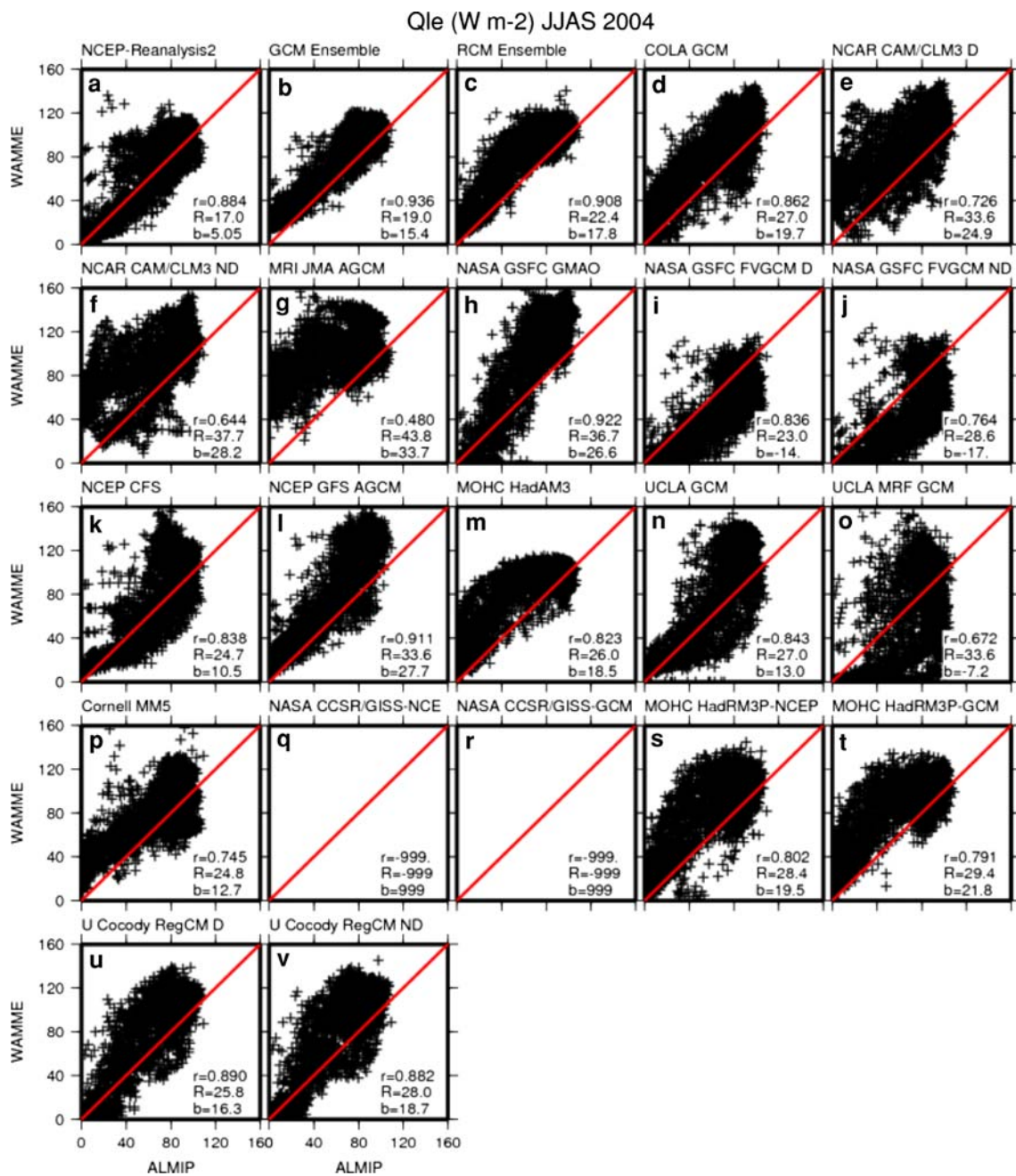


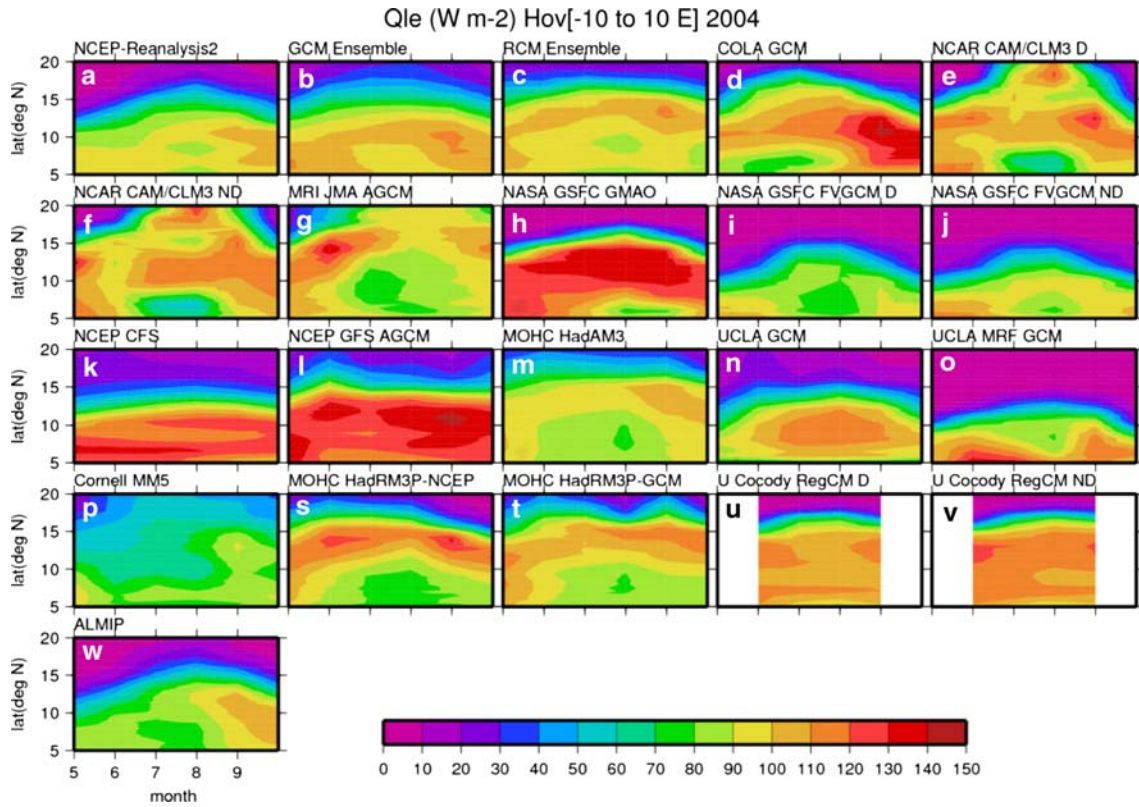
Fig. 9 As in Fig. 4 except for the latent heat flux

compared to ALMIP (owing to rainfall); however, SWIP values are nearly unity in a large area south of 10°N. In fact, this is a common trait in most of the WAMME models. In contrast, Kohler et al. (2009) showed that at a site located in Burkina Fasso (approximately 10° and -3°) during the special observing period in 2006, the daily average Bowen ratio (ratio of sensible to latent heat flux) tended to have minimum values after rainfall events no lower than about 0.27, which corresponds to a maximum SWIP as defined here of approximately 0.78 (consistent with the ALMIP values, which are less than 0.8). This

indicates that significant sensible heating of the atmosphere still takes place south of 10°N during the monsoon season in contrast to what is seen in the majority of WAMME models.

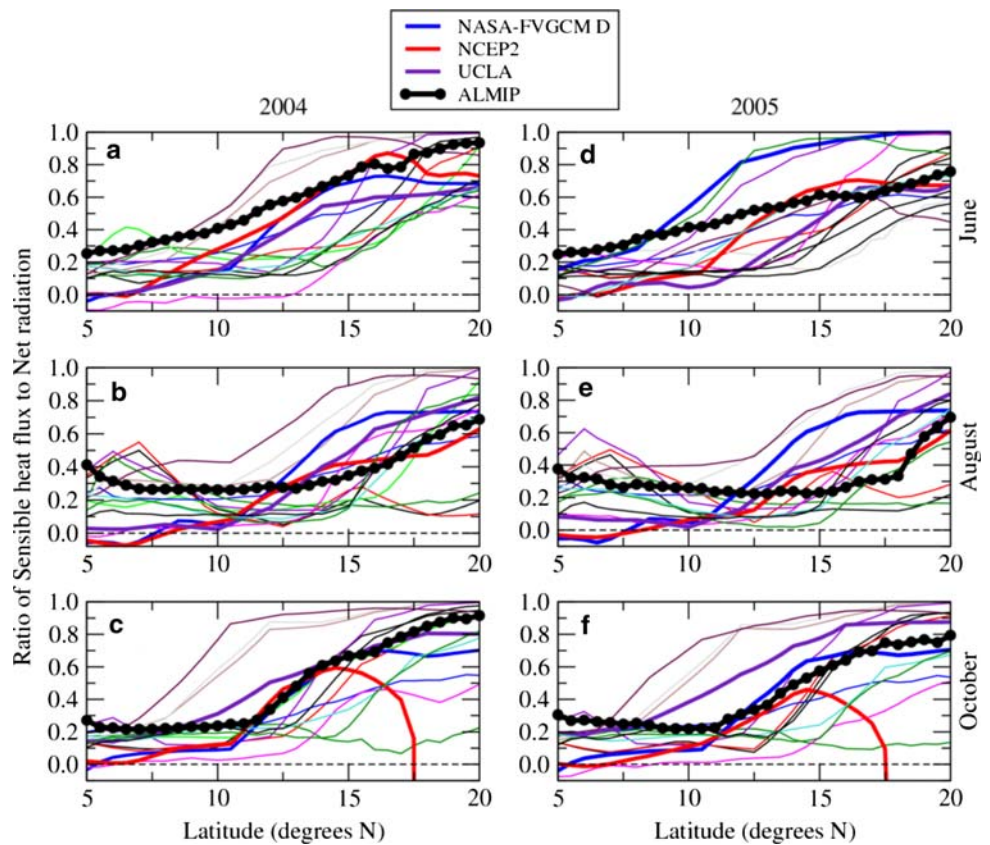
#### 4 Conclusions and perspectives

Surface energy fluxes simulated by an ensemble of land surface models from ALMIP have been used as a proxy for the best estimate of the “real world” values in order to



**Fig. 10** WAMME model latent heat flux Hovmoller plots for 2004 averaged from  $-10^{\circ}$  to  $10^{\circ}$ E for 2004. The ALMIP Hovmoller is shown in panel w

**Fig. 11** Meridional profiles of the ratio of the sensible heat flux to the net radiation for three different months averaged from  $-10^{\circ}$  to  $10^{\circ}$ E. The *thick black curve* corresponds to ALMIP. Several WAMME models are indicated



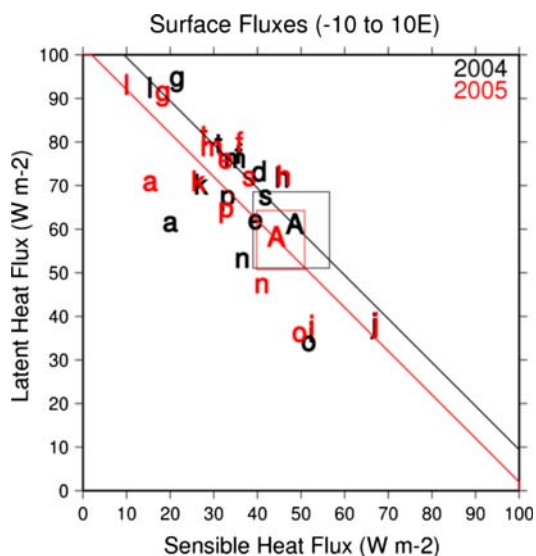


**Fig. 12** A comparison of the latent and sensible heat fluxes averaged from  $-10^{\circ}$  to  $10^{\circ}$ E and from May through October. The WAMME symbols are the same as those in Fig. 8. The A is used to indicate ALMIP. Boxes represent the ALMIP range. Diagonal lines represent the net radiation simulated by ALMIP

evaluate GCM and RCM simulations under the auspices of the WAMME project, since such large-scale observations do not exist. The ALMIP models have been forced in off-line mode using satellite and gauge based precipitation

estimates from TRMM 3B42, downwelling satellite based radiative flux products from OSI and LAND-SAF, and atmospheric state variables from NWP.

An ensemble average is computed for all of the surface energy and water budget components, and the inter-model variability is examined for two annual cycles. The LSM fluxes agree well with a coefficient of variation for latent heat flux ranging from approximately 5–15% over most of West Africa, with the best agreement over the semi-arid Sahel where precipitation recycling is most significant. The ensemble signal to noise ratio of the surface turbulent fluxes is fairly large over most of the region, with the exception of the equatorial rain forest. This is related to the fact that soils are deepest (impacting hydrology and water storage) and vegetation processes (such as radiative transfer and root zone water uptake) and interactions with the under story are more complex. The simulated fluxes over this region have a larger uncertainty (owing to more model disagreement), however, the focus is on the WAM so that the WAMME analysis is mostly done outside of this area.

The WAMME model simulated net radiation agrees rather well with ALMIP for most of the WAMME models, however, the partitioning of this energy into turbulent fluxes is different from ALMIP and is quite variable. The main reason for the difference with respect to ALMIP is that the WAMME models have a positive precipitation bias compared to ALMIP. Because there is ample energy, this leads

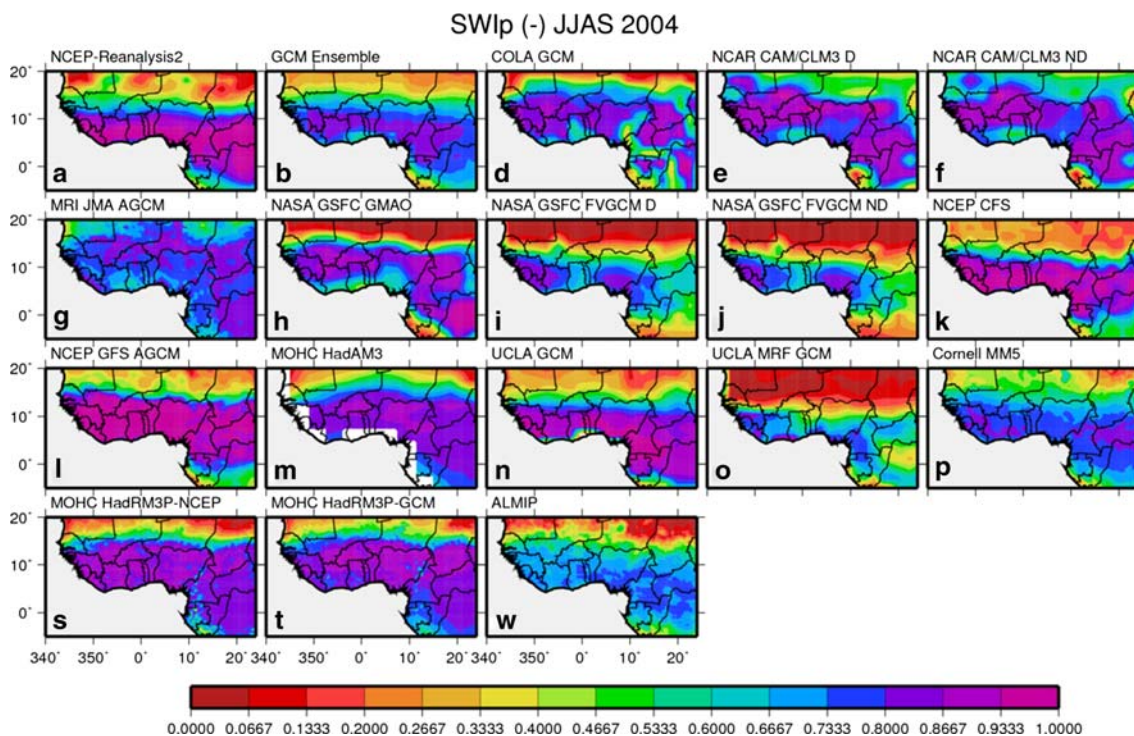


**Fig. 13** The WAMME Soil Wetness Index proxy (SWIp) averaged from June through September (JJAS) for 2004. The corresponding ALMIP field is shown in panel w

to larger latent heat fluxes and very little rainfall is being stored or becomes runoff in the WAMME models. This seems to be due, in part, to further northward placement of monsoon in areas with larger potential energy for evaporation or most of the WAMME models. Further research is needed to determine how much the surface contributes to this displacement of the WAM in the WAMME models. NCEP2 is a special case. Surface latent heat fluxes agree well with ALMIP compared to most of the WAMME models, which is comforting since, like ALMIP, the precipitation is not based on NWP (but rather a mixed satellite-gauge approach). But the surface net radiation is quite different (primarily owing to albedo differences), so that sensible heat fluxes are among the lowest of all the WAMME models (and in contrast to ALMIP estimates).

In terms of the annual cycle over West Africa, ALMIP produces the maximum latent heat flux during the monsoon retreat as stored water is evaporated before solar radiation reaches the boreal winter minima: only six of the WAMME models have this feature, and it is generally rather weak. Also, the starting point for the monsoon (in May) is further north than ALMIP for all of the WAMME models except for the two models which keep the monsoon too far south. Thus before onset, the maximum low level MSE gradient is further to the north than ALMIP for most of the WAMME models.

The meridional ratio of sensible heat flux to the net radiation during onset (June) (from 5° to 20°N) is larger in ALMIP than in the WAMME models, mainly because the monsoon starts further south and temporally lags most of the WAMME models (the monsoon jump in TRMM is generally more rapid than in the WAMME models). The best general agreement with ALMIP is in August, when the meridional gradient is generally the lowest. During the monsoon retreat, most of the WAMME models agree quite well with ALMIP south of 10°N (the aforementioned ratio is between 0.1 and 0.2 for most models), while north of 10°N there is the greatest dispersion of WAMME models for the 3 months considered. This seems to be related to large differences in soil water storage and its extraction within the WAMME models.

In order to truly respond to questions regarding the coupling between the land surface and the atmosphere using GCMs and RCMs, special experiments in which the models are constrained by offline soil moisture (e.g. Douville et al. 2001) or offline surface fluxes (perhaps using a flux replacement method, such as that presented by Dirmeyer and Zhao 2004) should be done focusing on this region using a multi-model GCM or RCM approach together with ALMIP outputs. This effort would also be complemented by the large unique dataset consisting in both surface and atmospheric data measured during the AMMA field campaign.

**Acknowledgments** The authors would like to acknowledge the support of the data providers, notably R. Lacaze, B. Geiger, D. Carrer and J.-L. Roujean, who have offered considerable assistance with respect to using the LAND-SAF downwelling radiative flux products. A. Marsouin provided guidance on the OSI-SAF radiation product. We wish to extend our gratitude to the POSTEL Service Centre (<http://postel.mediasfrance.org>) at MEDIAS-France for customising and providing the LSA SAF products. We gratefully acknowledge the European Centre for Medium-Range Weather Forecasts for the use of the ECMWF forecast data. We would like to acknowledge the hard work of the ALMIP Working Group members: G. Balsamo, A. Beljaars, C. Delire, P. Harris, C. Taylor, T. Orgeval, J. Polcher, A. Ducharne, A. Nørgaard, I. Sandholt, S. Gascoïn, Y. Gusev, O. Nasonova, S. Saux-Picart, C. Ottlé, and B. Decharme, and the WAMME Working Group members. Based on a French initiative, AMMA has been established by an international group and is currently funded by a large number of agencies, especially from France, the UK, and Africa. It has been the beneficiary of a major financial contribution from the European Community's Sixth Framework Research Programme.

## References

- Adler RF, Huffman GJ, Chang A, Ferraro R, Xie P, Janowiak J, Rudolf B, Schneider U, Curtis S, Bolvin D, Gruber A, Susskind J, Arkin P (2003) The Version 2 Global Precipitation Climatology Project (GPCP) monthly precipitation analysis (1979–present). *J Hydrometeorol* 4:1147–1167
- Balsamo G, Viterbo P, Beljaars A, van den Hurk B, Hirsch M, Betts A, Scipal K (2009) A revised hydrology for the ECMWF model: verification from field site to terrestrial water storage and impact in the Integrated Forecast System. *J Hydrometeorol* 10:623–643
- Boone A, Masson V, Meyers T, Noilhan J (2000) The influence of the inclusion of soil freezing on simulations by a soil–vegetation–atmosphere transfer scheme. *J Appl Meteorol* 9:1544–1569
- Boone A, de Rosnay P, Basalmo G, Beljaars A, Chopin F, Decharme B, Delire C, Ducharne A, Gascoïn S, Grippa M, Guichard F, Gusev Y, Harris P, Jarlan L, Kergoat L, Mougin E, Nasonova O, Nørgaard A, Orgeval T, Ottlé C, Pocard-Leclercq I, Polcher J, Sandholt I, Saux-Picart S, Taylor C, Xue Y (2009) The AMMA land surface model intercomparison project. *Bull Amer Meteorol Soc.* doi:10.1175/2009BAMS2786.1
- Charney J, Stone PH, Quirk WJ (1975) Drought in the Sahara: a biogeophysical feedback mechanism. *Science* 187:434–435
- Chen F, Dudhia J (2001) Coupling an advanced land surface–hydrology model with the Penn State-NCAR MM5 modelling system. Part I: model implementation and sensitivity. *Mon Weather Rev* 129:569–585
- Coudert B, Ottlé C, Boudevillain B, Guillevic P, Demarty J (2006) Contribution of thermal infrared remote sensing data in multi-objective calibration of a dual source SVAT model. *J Hydro-meteorol* 7:404–420
- Cunnington WM, Rowntree PR (1986) Simulations of the Saharan atmosphere—dependence on moisture and albedo. *Q J R Meteorol Soc* 112:971–999
- d'Orgeval T, Polcher J, de Rosnay P (2008) Sensitivity of the West African hydrological cycle in ORCHIDEE to infiltration processes. *Hydrol Earth Syst Sci Discuss* 5:2251–2292
- Dai Y, Zeng X, Dickinson RE, Baker I, Bonan GB, Bosilovich MG, Denning AS, Dirmeyer PA, Houser PR, Niu G, Oleson KW, Schlosser CA, Yang Z-L (2003) The common land model. *Bull Am Meteorol Soc* 84:1013–1023
- de Rosnay P, Polcher J, Bruen M, Laval K (2002) Impact of a physically based soil water flow and soil–plant interaction

- representation for modeling large scale land surface processes. *J Geophys Res* 107(D11), 4118. doi:[10.1029/2001JD000634](https://doi.org/10.1029/2001JD000634)
- de Rosnay P, Drusch M, Boone A, Balsamo G, Decharme B, Harris P, Kerr Y, Pellarin T, Polcher J, Wigneron JP (2009) Microwave Land Surface modelling evaluation against AMSR-E data over West Africa. The AMMA Land Surface Model Intercomparison Experiment coupled to the Community Microwave Emission Model (ALMIP-MEM). *J Geophys Res* 114, D05108. doi:[10.1029/2008JD010724](https://doi.org/10.1029/2008JD010724)
- Decharme B (2007) Influence of the runoff representation on continental hydrology using the NOAH and the ISBA land surface models. *J Geophys Res* 112:D19108. doi:[10.1029/2007JD008463](https://doi.org/10.1029/2007JD008463)
- Dickinson RE, Henderson-Sellers A, Kennedy PJ (1993) Biosphere–Atmosphere Transfer Scheme (BATS) version 1e as coupled to the NCAR Community Climate Model. NCAR Technical Note NCAR/TN-387 + STR, 72
- Dirmeyer PA, Zhao M (2004) Flux replacement as a method to diagnose coupled land–atmosphere model feedback. *J Hydrometeorol* 5:1034–1048
- Dirmeyer PA, Dolman AJ, Sato N (1999) The pilot phase of the Global Soil Wetness Project. *Bull Am Meteorol Soc* 80:851–878
- Dirmeyer PA, Gao X, Zhao M, Guo Z, Oki T, Hanasaki N (2006) GSWP-2: multimodel analysis and implications for our perception of the land surface. *Bull Am Meteorol Soc* 87:1381–1397
- Douville H, Chauvin F, Broqua H (2001) Influence of soil moisture on the Asian and African monsoons. Part I: mean monsoon and daily precipitation. *J Clim* 14:2381–2403
- Douville H, Conil S, Tyteca S, Voldoire A (2007) Soil moisture memory and West African monsoon predictability: artefact or reality? *Clim Dyn* 28:723–742
- Eltahir EAB, Gong C (1996) Dynamics of wet and dry years in West Africa. *J Clim* 9:1030–1042
- Essery RLH, Best M, Betts R, Cox P, Taylor CM (2003) Explicit representation of subgrid heterogeneity in a GCM land surface scheme. *J Hydrometeorol* 4:530–543
- Gao X, Dirmeyer PA (2006) A multimodel analysis, validation, and transferability study of global soil wetness products. *J Hydrometeorol* 7:1218–1236
- Geiger B, Meurey C, Lajas D, Franchistguy L, Carrer D, Roujean J-L (2008) Near real-time provision of downwelling shortwave radiation estimates derived from satellite observations. *Meteorol Appl* 15:411–420
- Guo Z, Dirmeyer PA, Koster RD, Bonan G, Chan E, Cox P, Gordon CT, Kanae S, Kowalczyk E, Lawrence D, Liu P, Lu C-H, Malyshev S, McAvaney B, McGregor JL, Mitchell K, Mocko D, Oki T, Oleson KW, Pitman A, Sud YC, Taylor CM, Verseghy D, Vasic R, Xue Y, Yamada T (2006) GLACE: the global land–atmosphere coupling experiment. Part II: analysis. *J Hydrometeorol* 7:611–625
- Gusev EM, Nasonova ON, Kovalev EE (2006) Modeling the components of heat and water balance for the land surface of the globe. *Water Resour* 33:616–627
- Henderson-Sellers A, Pitman A, Love P, Irannejad P, Chen T (1995) The project for intercomparison of land surface parameterization schemes (PILPS): phases 2 and 3. *Bull Amer Meteor Soc* 76:489–504
- Hourdin F, Guichard F, Favot F, Marquet P, Boone A, Lafore J-P, Redelsperger J-L, Ruti P, Dell’Aquila A, Doval TL, Traore AK, Gallee H (2009) AMMA-Model Intercomparison Project. *Bull Am Meteorol Soc* (in press)
- Huffman GJ, Adler RF, Bolvin DT, Gu G, Nelkin EJ, Bowman KP, Hong Y, Stocker EF, Wolff DB (2007) The TRMM multi-satellite precipitation analysis: Quasi-global, multi-year, combined-sensor precipitation estimates at fine scale. *J Hydrometeorol* 8:38–55
- Jobard I, Chopin F, Bergés JC, Ali A, Lebel T, Desbois M (2007) Presentation of the EPSAT-SG method and comparison with other satellite precipitation estimations in the frame of Precip-AMMA. *Geophysical Research Abstracts*, vol 9, 10062, SRef-ID: 1607–7962/gra/EGU2007-A-10062. European Geosciences Union
- Kang H-S, Xue Y, Collatz G (2007) Impact assessment of satellite-derived leaf area index datasets using a general circulation model. *J Clim* 20:993–1013
- Kohler M, Kalthoff N, Kottmeier C (2009) The impact of soil moisture modifications on CBL characteristics in West Africa: a case study from the AMMA campaign. *QJR Meteorol Soc* (in press). doi:[10.1002/qj.430](https://doi.org/10.1002/qj.430)
- Koster RD, Suarez MJ (1996) Energy and water balance calculations in the MOSAIC LSM. NASA Technical Memorandum 104606, 9, 76
- Koster RD, Suarez MJ, Ducharme A, Kumar P, Stieglitz M (2000) A catchment-based approach to modeling land surface processes in a GCM—Part 1: model structure. *J Geophys Res* 105:24809–24822
- Koster RD, Dirmeyer PA, Hahmann AN, Ijpehaar R, Tyahla L, Cox P, Suarez MJ (2002) Comparing the degree of land–atmosphere interaction in four atmospheric general circulation models. *J Hydrometeorol* 3:363–375
- Koster RD, Guo Z, Dirmeyer PA, Bonan G, Chan E, Cox P, Davies H, Gordon CT, Kanae S, Kowalczyk E, Lawrence D, Liu P, Lu C-H, Malyshev S, McAvaney B, Mitchell K, Mocko D, Oki T, Oleson KW, Pitman A, Sud YC, Taylor CM, Verseghy D, Vasic R, Xue Y, Yamada T (2006) GLACE: the global land–atmosphere coupling experiment. Part I: overview. *J Hydrometeorol* 7:590–610
- Koster RD, Guo Z, Yang R, Dirmeyer PA, Mitchell K, Puma MJ (2009) On the nature of soil moisture in land surface models. *J Clim* (in press). doi:[10.1175/2009JCLI2832.1](https://doi.org/10.1175/2009JCLI2832.1)
- Laval K, Picon L (1986) Effect of a change of the surface albedo of the sahel on climate. *J Atmos Sci* 43:2418–2429
- Laws KB, JE Janowiak, GJ Huffman (2004) Verification of rainfall estimates over Africa using RFE, NASA MPA-RT and CMORPH. In: American Meteorological Society 18th Conference on Hydrology, Seattle, WA, January 2004
- Li W, Xue Y, Pocard I (2007) Numerical investigation of the impact of vegetation indices on the variability of West African summer monsoon. *J Meteorol Soc Jpn* 85:363–383
- Masson V, Champeaux J-L, Chauvin F, Meriguet C, Lacaze R (2003) Global database of land surface parameters at 1-km resolution in meteorological and climate models. *J Clim* 16:1261–1282
- Noilhan J, Mahfouf J-F (1996) The ISBA land surface parameterization scheme. *Glob Planet Change* 13:145–159
- Pan H-L, Mahrt L (1987) Interaction between soil hydrology and boundary layer developments. *Boundary Layer Meteorol* 38:185–202
- Parker DJ, Thorncroft CD, Burton RR, Diongue-Niang A (2005) Analysis of the African easterly jet, using aircraft observations from the JET2000 experiment. *Q J R Meteorol Soc* 131:1461–1482
- Philippon N, Fontaine B (2002) The relationship between the Sahelian and previous 2nd Guinean rainy seasons: a monsoon regulation by soil wetness? *Ann Geophys* 20:575–582
- Redelsperger J-L, Thorncroft CD, Diedhiou A, Lebel T, Parker DJ, Polcher J (2006) African Monsoon Multidisciplinary Analysis: an international research project and field campaign. *Bull Am Meteorol Soc* 87:1739–1746
- Rosenzweig C, Abramopoulos F (1997) Land-surface model development for the GISS GCM. *J Clim* 10:2040–2054
- Rowell DP, Blondin C (1990) The influence of soil wetness distribution on short range rainfall forecasting in the West African Sahel. *Q J R Meteorol Soc* 116:1471–1485

- Schneider U, Fuchs T, Meyer-Christoffer A, Rudolf B (2008) Global precipitation analysis products of the GPCC. Global Precipitation Climatology Centre (GPCC), DWD, Internet Publikation, 1–12
- Sellers PJ, Mintz Y, Dalcher A (1986) A simple biosphere model (SiB) for use within general circulation models. *J Atmos Sci* 43:505–531
- Steiner AL, JS Pal, SA Rauscher, JL Bell, NS Diffenbaugh, A Boone, LC Sloan, F Giorgi (2009) Land surface coupling in a regional climate simulations of the West African monsoon. *Clim Dyn*. doi [10.1007/s00382-009-0543-6](https://doi.org/10.1007/s00382-009-0543-6)
- Sud YC, Fennessy M (1982) A study of the influence of surface albedo on July circulation in semi-arid regions using the GLAS GCM. *J Climatol* 2:105–125
- Timouk F, L Kergoat, E Mougin, C Lloyd, E Ceschia, P de Rosnay, P Hiernaux, V Demarez (2008) Response of sensible heat flux to water regime and vegetation development in a central Sahelian landscape. *J Hydrol* 1–43. doi: [10.1016/j.jhydrol.2009.04.022](https://doi.org/10.1016/j.jhydrol.2009.04.022)
- Walker J, Rowntree PR (1977) The effect of soil moisture on circulation and rainfall in a tropical model. *Q J R Meteorol Soc* 77:353–378
- Xue Y, Shukla J (1996) The influence of land surface properties on Sahel climate. Part II: afforestation. *J Clim* 9:3260–3275
- Xue Y, Sellers PJ, Kinter JL III, Shukla J (1991) A simplified biosphere model for global climate studies. *J Clim* 4:345–364
- Xue Y, Hutjes RWA, Harding RJ, Claussen M, Prince SD, Lebel T, Lambin EF, Allen SJ, Dirmeyer PA, Oki T (2004) The Sahelian climate. Vegetation, water, humans and the climate: a new perspective on an interactive system. Springer, Heidelberg, pp 59–78
- Xue Y, K-M Lau, KH Cook, D Rowell, A Boone, J Feng, T Bruecher, FDe Sales, P Dirmeyer, LM Druyan, A Fink, M Fulakeza, Z Guo, S M Hagos, SS Ibrah, K-M Kim, A Kitoh, A Konare, V KumarI, P Lonergan, M PasquiI, I Pocard-Leclercq, N Mahowald, W Moufouma-Okia, P Pegion, JK Schemm, SD Schubert, A Sealy, WM Thiaw, A Vintzileos, EK Vizy, S Williams, M-L C Wu (2009) The West African Monsoon Modeling and Evaluation project (WAMME) and its First Model Intercomparison Experiment. *Clim Dyn* (under revision)
- Zeng N, Neelin J, Lau K-M, Compton J (1999) Enhancement of interdecadal climate variability in the Sahel by vegetation interaction. *Science* 286:1537–1540